Image Simulation Technique Human Brain

Dr.P.K.Subudhi [1], Himanshu Bhusan Mohapatra [2] S Behera [3]

[1] Professor, Department of Electronics and Communication Engineering, Gandhi Institute For Technology (GIFT), Bhubaneswar

[2] Assistant Professor, Department of Electronics and Communication Engineering, Gandhi Engineering College, Bhubaneswar

[3] Assistant Professor, Department of Electronics and Communication Engineering, Gandhi Institute For Technology (GIFT), Bhubaneswar

Abstract: Two novel preprocessing techniques are applied to reinforce the detection performance and the image quality in microwave imaging systems designed for brain stroke detec- tion. The image of energy distribution is obtained by applying a delay-and-sum beamforming to the backscattered signals mea- sured using a hemielliptical array of 16 corrugated tapered slot antenna elements surrounding the head. The beamformer forms a spatially filtered combination of time-delayed response of scat- tering points in the head exposed to microwave radiation over the band from 1 to 4 GHz. The proposed techniques are validated on a realistic head phantom that is fabricated to emulate the electrical properties of real human head. The results show how the proposed techniques enable the detection and localization of hemorrhagic stroke accurately.

Index Terms: Brain stroke detection, delay-and-sum beam- forming, head phantom, microwave imaging.

I. INTRODUCTION

A BRAIN stroke is the rapid loss of brain functions due to disturbance in the blood supply. The stroke can be due to ischemia or a hemorrhage. A patient suffering from a suspected stroke is a medical emergency. Its symptoms typically start sud- denly and possibly cause permanent neurological damage, com- plications, and death. The risk factors for stroke include old age, hypertension, or transient ischemic attack, diabetes, high cholesterol, cigarette smoking, and atrial fibrillation [1].

Currently, physicians rely on computed tomography (CT) and magnetic resonance imaging (MRI) for stroke identification. CT can confirm the diagnosis of stroke and tell whether the stroke is caused by a hemorrhage in the brain. MRI is used to identify and further localize the site of the stroke and find the source. It may be able to quickly identify the ischemic stroke. However, these two tools are costly and not always accessible. They are also not portable and thus cannot be carried by first-response paramedical teams [2].

Microwave imaging is a promising candidate for biomedical applications as it can create a map of electromagnetic wave scat- tering arising from the contrast in the dielectric properties of dif- ferent tissues [3]–[6]. Microwave imaging has been investigated as a possible low-cost and portable imaging modality for stroke identification by the first response paramedics. Recent studies have demonstrated that the two types of brain stroke (hemorrhagic and ischemic) significantly change the dielectric proper- ties of the affected tissues at microwave frequency [2], [7].

In this letter, we propose novel techniques for efficient pre- processing algorithms to remove the background signals and thereby to achieve accurate detection and localization of brain stroke. The proposed techniques are tested with the well-known delay-and-sum beamforming for spatially focusing the scattered signals. The accuracy of preprocessing methods to determine the time-delayed response of the target object is validated using a realistic 3-D head phantom with appropriate electrical prop- erties and a monostatic radar system that uses a hemielliptical antenna array with 16 antennas.

II. IMAGING ALGORITHM

The confocal microwave imaging is a promising and at- tractive reconstruction method. It quantitatively computes the spatial distributions of the dielectric constant and/or conduc- tivity [8]. In this letter, wideband confocal modality based on delay-and-sum beamforming is considered by using the backscattered signals at different antenna locations to calculate the energy distribution coherently.

A.   Signal Preprocessing

The backscattered data is acquired using a monostatic an- tenna array. Since a strong background reflection dominates the reflected signal, signal preprocessing is essential. It com- monly comprises extracting the target response at each antenna location.

In breast imaging, the reflections at the free space–breast interface are removed by subtracting the average reflected signal from each captured signal [8]. However, the background reflections in the different channels of head imaging system are not identical mainly due to the hemiellipsoidal shape of the head and its heterogeneity. Thus, subtracting the average across all the array elements does not eliminate those reflections. More sophisticated algorithms [9] achieve better results on breast microwave imaging. Two approaches with low computational overhead and efficient performance are presented here.

The signal transmission and reception are performed in the frequency domain. The received signal at the th channel is con- verted to sampled waveform and transformed into a positive valued samples in the time domain , where denotes the antenna array size) and .Based on two new approaches in this letter, the background reflections are eliminated to construct the target response that shows up at different time shifts. To perform the stroke de- tection and optimize the beamformer's performance, the back- ground reflections are removed by determining the difference in scattered signals using one of the following two approaches. A schematic model for the head phantom and array elements is depicted in Fig. 1.
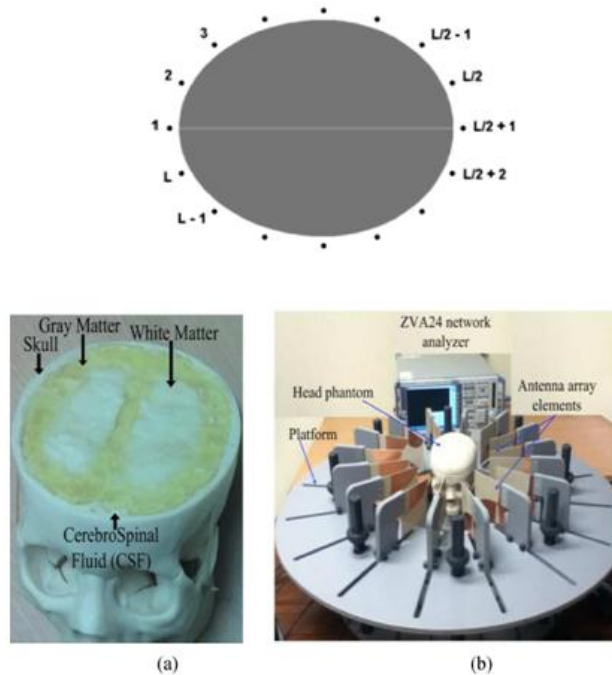
Fig. 1. Microwave imaging setup. The gray shaded hemielliptical area presents the head, and the discrete points L denote antenna array elements.

Since the human head is anatomically symmetrical with respect to the central line that divides the head into left and right halves, the background signals, such as free space–head phantom interface reflections, are almost identical with same time position in channels facing each other in the symmet- rical array. Upon testing healthy brain, the backscattered signals at antennas facing each other in the array, i.e., ζ_n^i and $\zeta_n^{(L-i+2)\bmod L}$, are identical. Fig. 1 portrays the arrangement of the antenna elements in the array.
Thereby, to test the presence of abnormal target, we construct the difference signal based either on App-A or App-B that are explained hereafter.

1)   First Approach (App-A): Based on the first proposed ap- proach, the difference signal is constructed by the subtraction of backscattered signal pairs as given by

$$\mathrm{d}_n^i = \zeta_n^i - \zeta_n^{i-1} \qquad (1)$$

$$\mathrm{d}_n^{\frac{L}{2}+i} = \zeta_n^{\frac{L}{2}+i} - \zeta_n^{\frac{L}{2}+i+1}$$

$$(2)$$

for $i = 1, 2, \ldots (L/2)$ where $\zeta_n^0 = \zeta_n^L$ and $\zeta_n^{L+1} = \zeta_n^1$. Based on antenna array of 16 elements, for example, the target response at the antenna 3 $d_n^3 = \zeta_n^3 - \zeta_n^2$, and the target response at antenna $i = 15$ $d_n^{15} = \zeta_n^{15} - \zeta_n^{16}$ is

2) Second Approach (App-B): Based on the symmetrical dis- tribution of brain tissues in the right and left sides, it is possible to consider a differential approach in which the background re- flection is removed by using the difference backscattered signals as given by

$$d_n^i = \zeta_n^i - \zeta_n^{(L-i+2)\bmod L} \tag{3}$$

for $i = 1, 2, \ldots L$. For example, in an antenna array of 16 el- ements $d_n^7 = \zeta_n^7 - \zeta_n^{11} = -d_n^{11}$. Next, the negative-valued samples of the differential signals are replaced by zeros to avoid getting mirror or ghost targets.

The results in the next section show that these approaches highly reinforce the target response while the unwanted off-axis scattering response is removed. The higher-quality microwave images validate our claim.

B. Delay-and-Sum Beamforming

Beamforming or spatial filtering is used for directional signal transmission or reception to achieve spatial selectivity. It com- bines elements in an antenna array such that signals experi- ence either constructive or destructive interference at particular angles.

A conventional beamformer can be a simple delay-and-sum with a fixed set of weightings or a more sophisticated adaptive beamformer with a time and spatial variant weightings. In this letter, a delay-and-sum beamformer is applied using primarily

Fig. 2. (a) Cross section of head phantom and (b) imaging system.

the wave directions of interest, the location of the antennas in space, and the wave propagation speed $c/\sqrt{\varepsilon_{av}}$, where is the speed of electromagnetic wave in free space and is the av- erage dielectric constant of the tissues inside head. is taken here as 40, which is the average dielectric constant of the two main tissues inside the human head, i.e., the white and gray matters.

The beamformer is steered to a specified direction by se- lecting appropriate phases for each antenna. It aligns the return from each scattering point (as a focal point's response) to the radiated signal from each antenna's location.

The spatial focusing is achieved by determining the time position in the captured signals. Finally, coherent summation of all the responses is performed to find the intensity distribution. A map of energy spatial distribution provides an image of backscattered signals' strength.

In order to compute the time position of each focal point's response, it is necessary to find the most probable path that the electromagnetic wave travels from an antenna source to the point. The least-time principle is applied here, which states that the correct path is the shortest electrical distance the wave would travel.

The images in Section IV demonstrate the effectiveness of the simple background removal processing and the delay-and-sum beamforming by applying them to the measured backscattered signals.

III. MEASUREMENT SETUP

To test the proposed techniques, a realistic 3-D head phantom [Fig. 2(a)] with electrical properties that perfectly emulate those of real head tissues is fabricated based on the available data [10]. In the fabrication, suitable mixtures of water, corn flour, gelatin, agar, sodium azide, and propylene glycol are used to form the different tissues of the brain and to account for the frequency- dependent properties of the brain tissues [11]. Using the di- electric probe HP85070, we confirmed that the properties of the fabricated tissues agree with the realistic properties pub- lished in [10] with less than 3% error across the band from 1 to 4 GHz. The measurements were also repeated two months after the phantom's fabrication to confirm the stability of the proper- ties over time. To emulate a hemorrhagic stroke region, an el- lipsoid object with radii of 14 7 mm and thickness of 5 mm is also fabricated and inserted inside the phantom at different locations. Since the hemorrhagic stroke is caused by bleeding, the electrical properties of that stroke are equivalent to blood.

The head phantom is exposed to wideband microwave signal covering the frequency band from 1 to 4 GHz. This band is se- lected as a suitable compromise between the required resolution and signal penetration. The signal is generated synthetically by a swept frequency input. The signal transmission and recep- tion is done using a monostatic radar system based on a real aperture hemielliptical antenna array. The array is formed using corrugated tapered slot antennas that are distributed around the head phantom. The antennas are designed using the guidelines presented in [12] and [13]. Each of the fabricated antennas has the dimensions of 9.4 11 cm .

They are built on the substrate Rogers RT3010 with dielectric constant of 10.2 and thickness of 1.28 mm. The measured reflection coefficient of one of those antennas and the mutual coupling between any two neighboring elements are depicted in Fig. 3. The developed antennas have less than 10 dB reflection coefficient across the band from 1 to 4 GHz. The mutual coupling between any two antenna ele- ments forming the array is less than 20 dB across the same band.

As a compromise between the need for a large number of an- tennas to get sufficient information about the target and the need to have a reasonable distance between those antennas for a low mutual coupling, 16 equally distributed antennas are used with a fixed distance of 5 mm from the head boundary [Fig. 2(b)]. In order to investigate the effect of increasing the number of antennas to 32 without increasing the mutual coupling between them, the measurements are taken from the 16 elements, and then the platform is rotated by an angle of $360/32$. Another set of measurements is taken. The combined two sets represent the case of using 32 antenna elements. All the mea- surements are performed in the frequency domain using a stan- dard vector network analyzer.
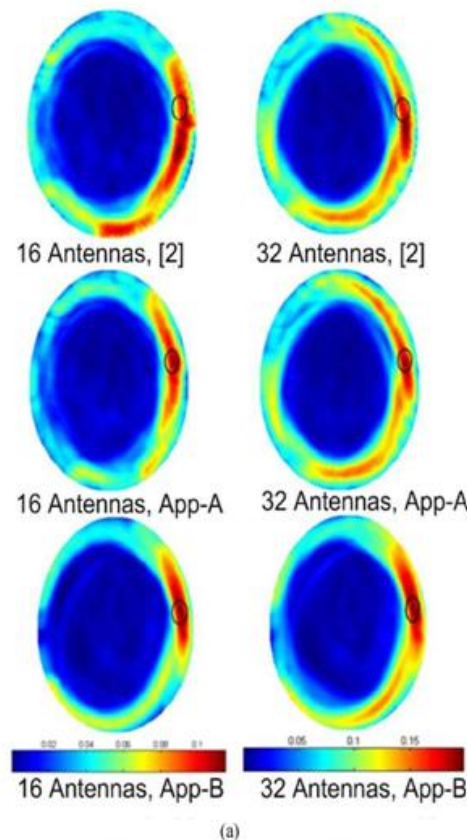
$$= 11.25°$$

IV.   RESULTS

The overall performance of microwave imaging via delay- and-sum beamforming is evaluated based on each described ap- proach in Section II for strong background reflection removal. The brain stroke is monitored using the microwave frequency range 1–4 GHz, which is used as a reasonable compromise be- tween the required imaging resolution and head penetration. App-A and App-B are used to denote the first and second ap- proaches, respectively. The performance is compared to that ap- plied in [2], which is based on antenna rotation/background sub- traction followed by a compensation for the signal loss.

The images from applying the three different techniques are depicted in Fig. 4 for two different realistic locations of stroke. It is clear from the presented results that the focusing performance is compromised when the background removal is not carried out successfully as in [2], especially with smaller array size. When the proposed method (App-B) is applied, the stroke is accurately detected and localized for the two investigated cases.

Tables I and II present the value of quantitative metrics de- fined in [2] and used to quantify the effectiveness of the con- structed head images of Fig. 4(a) and (b). The metric Q is de- fined as the ratio of the average intensity in the actual stroke area to the average intensity in the rest of head tissues as given by
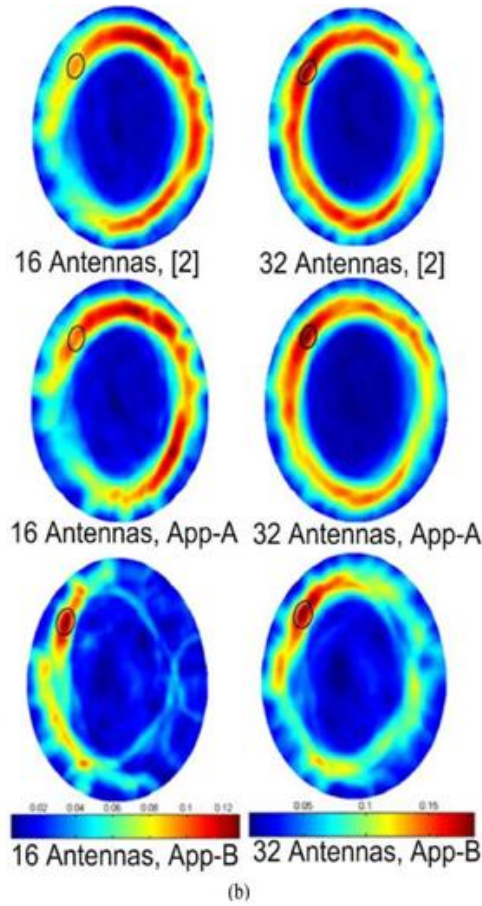

16 Antennas, [2]   32 Antennas, [2]

16 Antennas, App-A   32 Antennas, App-A

16 Antennas, App-B   32 Antennas, App-B

(a)

16 Antennas, [2]   32 Antennas, [2]

16 Antennas, App-A   32 Antennas, App-A

16 Antennas, App-B   32 Antennas, App-B

(b)

TABLE I
QUANTITATIVE METRICS FOR THE MICROWAVE IMAGES IN FIG. 4(a)

	Q	φ	$\Delta(cm)$
[2]	2.71/2.49	0.98/1.01	3.26/0.96
App-A	3.155/2.53	1.15/1.13	0.158/0.158
App-B	3.88/3.22	1.06/1.08	0.07/0.07

TABLE II
QUANTITATIVE METRICS FOR THE MICROWAVE IMAGES IN FIG. 4(b)

	Q	φ	$\Delta(cm)$
[2]	1.81/2.29	0.73/1.08	6/0.8
App-A	1.93/2.36	0.85/1.08	5/0.1
App-B	3.23/2.8	1.2/1.1	0.32/0.07

where $\mu[\cdot]$ denotes the mean value. S is the set of points form the detected target in the head, and is the set of all points within the head area. The second metric denotes the ratio of the maximum intensity in the stroke area to the maximum in- tensity in the head out of the stroke area. φ points to the failure in localizing the stroke since the focal point of maximum intensity is out of the stroke area. Furthermore, $\varphi > 1$ interprets the contrast in the computed maximum intensity $\varphi < 1$

$$\frac{\max[I(\boldsymbol{p})]}{\max[I(\boldsymbol{p})]} \quad \begin{array}{l} \forall \boldsymbol{p} \in \mathcal{S} \\ \forall \boldsymbol{p} \in \mathcal{H} \ \& \ \boldsymbol{p} \notin \mathcal{S} \end{array}. \quad (5)$$

The last metric is the distance between the real center and the predicted center of the stroke depending on the estimated maximum intensity given in the obtained map of energy distri- bution, as given by

$$\Delta = \|p^* - \chi\| \tag{6}$$

where $p^* = \underset{\boldsymbol{p} \in \boldsymbol{H}}{\mathrm{argmax}[I(\boldsymbol{p})]}$. Ideal imaging requires $\Delta = 0$.

The recorded results in Tables I and II show that App-B presents higher contrast in the stroke area compared to other approaches implemented in this letter, while the approach of [2] is the worst. Using [2] with an array size of 16 antennas fails to localize the stroke as illustrated in Table I. Using App-B with a large-size antenna array guarantees localizing the maximum intensity almost exactly inside the stroke area. With the highly lossy and heterogeneous nature of human head, the ideal zero value for is not easy to achieve. However, we successfully minimize its value using App-B.

The main goal of microwave imaging is either the detec- tion or localization of a target. It might also be both purposes. The importance of each metric depends on the purpose of the imaging. For the detection of an abnormal target, Q is the main metric to watch, whereas is the important metric for local- izing the target. The presented results validate our proposed ap- proaches. The results also indicate that App-A is less robust compared to App-B due to ignoring the neighboring channel-to- channel variations from the differences in skull thickness and head heterogeneity.

To show the capability of the proposed approaches to detect deep targets, an experiment is performed with a target that is located deep inside the head phantom. The results depicted in Fig. 5 using 32 antenna elements indicate that both of the pro- posed methods (App-A and App-B) are able to detect the target. However, the location of the detected target seems to be slightly
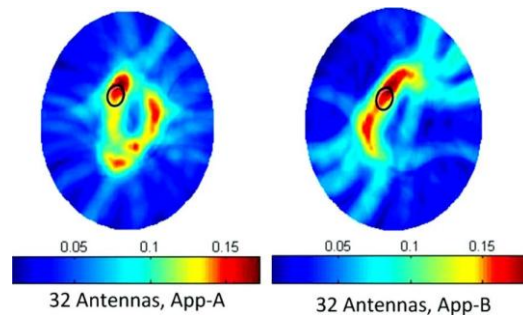
Fig. 5. Microwave brain imaging using antenna array of 32 elements. The el- lipcs with black color denotes the actual location of a deep stroke.

shifted from the exact location. Moreover, the size of the de- tected target by App-B seems to be larger than the assumed target.

V. CONCLUSION

Microwave systems for brain imaging have attracted our attention due to the importance of building a cost-effective, portable, and accessible tool to detect and localize brain strokes. To improve the performance of microwave systems for brain imaging, two novel approaches aimed to find the time delayed response of the stroke by efficiently removing the background scattered signals have been proposed. To quantify the image quality, three metrics have been used. The results on a realistic head phantom with an emulated hemorrhagic stroke demonstrate the efficacy of our approaches in the detection and localization of brain strokes.

REFERENCES

[1]. The Internet Stroke Center, Dallas, TX, USA, "The Internet Stroke Center," [Online]. Available: http://www.strokecenter.org/
[2]. D. Ireland and M. Bialkowski, "Microwave imaging for stroke detec- tion," *Prog. Electromagn. Res.*, vol. 21, pp. 163–175, 2011.
[3]. B. Mohammed, D. Ireland, and A. Abbosh, "Experimental inves- tigations into detection of breast tumour using microwave system with planar array," *Microw. Antennas Propag.*, vol. 6, no. 12, pp. 1311–1317, 2012.
[4]. A. Abbosh and S. Crozier, "Strain imaging of the breast by compres- sion microwave imaging," *IEEE Antennas Wireless Propag. Lett*, vol. 9, pp. 1229–1232, 2010.
[5]. R. Scapaticci, L. Di Donato, I. Catapano, and L. Crocco, "A feasibility study on microwave imaging for brain stroke monitoring," *Prog. Elec- tromagn. Res.*, vol. 40, pp. 305–324, 2012.
[6]. B. Mohammed, A. Abbosh, and D. Ireland, "Stroke detection based on variations in reflection coefficients of wideband antennas," in *Proc. IEEE Antennas Propag. Symp.*, Chicago, IL, USA, 2012, pp. 1–2.
[7]. Y. Serguei, Y. Semenov, and D. Corfield, "Microwave tomography for brain imaging: Feasibility assessment for stroke detection," *Int. J. Antennas Propag.*, vol. 2008, p. 254830, 2008.

[8]. E. Fear, X. Li, S. Hagness, and M. Stuchly, "Confocal microwave imaging for breast cancer detection: Localization of tumors in three dimensions," *IEEE Trans. Biomed. Eng.*, vol. 49, no. 8, pp. 812–822, Aug. 2002.

[9]. E. Bond, X. Li, S. Hagness, and B. Van Veen, "Microwave imaging via space-time beamforming for early detection of breast cancer," *IEEE Trans. Antennas Propag.*, vol. 51, no. 8, pp. 1690–1705, Aug. 2003.

[10]. S. Gabriel, R. Lau, and C. Gabriel, "The dielectric properties of bi- ological tissues: III. Parametric models for the dielectric spectrum of tissues," *Phys. Med. Biol.*, vol. 41, no. 11, pp. 2271–2293, 1996.

[11]. B. Mohammed, A. Abbosh, B. Henin, and P. Sharpe, "Head phantom for testing microwave systems for head imaging," in *Proc. Int. Biomed. Eng. Conf.*, Cairo, Egypt, Dec. 20–22, 2012, pp. 191–193.

[12]. A. Abbosh, H. Kan, and M. Bialkowski, "Design of compact directive ultra wideband antipodal antenna," *Microw. Opt. Technol. Lett.*, vol. 48, no. 12, pp. 2448–2450, 2006.

[13]. A. Abbosh, "Miniaturization of planar ultrawideband antenna via cor- rugation," *IEEE Antennas Wireless Propag. Lett.*, vol. 7, pp. 685–688, 2008.